ELSEVIER

Surface Science 423 (1999) 225–231

surface science

Photon- and electron-stimulated desorption of O^+ from zirconia

W.C. Simpson [a], W.K. Wang [b], J.A. Yarmoff [b], T.M. Orlando [a,*]

[a] *W.R. Wiley Environmental Molecular Sciences Laboratory, Pacific Northwest National Laboratory, P.O. Box 999, MS K8-88, Richland, WA 99352, USA*

[b] *Department of Physics, University of California, Riverside CA 92521 and Materials Sciences Division, Lawrence Berkeley National Laboratory, Berkeley, CA 94720, USA*

Received 27 July 1998; accepted for publication 24 November 1998

Abstract

We present a study of the photon- and electron-simulated desorption (PSD and ESD) of cations from yttria-stabilized cubic $ZrO_2(100)$ and undoped amorphous ZrO_2 surfaces. For both types of zirconia, O^+ is the primary ionic desorption product. A weak threshold for ESD of O^+ from yttria-stabilized cubic zirconia (YSZ) is observed at $\sim$26–27 eV with a rapid rise above $\sim$30 eV. The PSD threshold from YSZ is $\sim 31 \pm 1$ eV. This is essentially the same as the O^+ ESD and PSD thresholds ($\sim 30 \pm 1$ eV) from undoped amorphous ZrO_2 surfaces. The PSD O^+ kinetic energy distributions extend from 0 to $\sim$7 eV with a peak at $\sim$2 eV and are similar from both surfaces. A comparison of the ion threshold data with photoelectron spectra indicates that desorption of O^+ is primarily initiated by excitation of the Zr(4p) core level. All of the evidence is consistent with a desorption mechanism, in which the O^+ ions are produced and ejected from the surface via a multi-electron Auger decay process.

Keywords: Electron-stimulated desorption (ESD); Photon-stimulated desorption (PSD); ZrO_2 surfaces

1. Introduction

Zirconia (ZrO_2) is a wide-band-gap (>5 eV) refractory transition metal oxide that is used in a wide variety of applications, including high-temperature fuel cells, oxygen sensors and thermal barrier coatings [1,2]. Since zirconia is a maximally valent ionic material, it is expected to be highly resistant to damage by electromagnetic radiation and energetic particle bombardment. It is therefore used as a coating for high-power laser optics [3,4], and has been proposed as a substrate for radiation resistant electronic devices. In addition, it is the protective native oxide formed on nuclear fuels containing zirconium-alloy claddings [5].

In spite of the vast technological relevance of zirconia, there have been relatively few studies of the surface properties and radiation stability of ZrO_2 films and single-crystals. Past investigations have largely focused on understanding the kinetics and oxidation of Zr metal [6–21] and the interactions of adsorbates such as water [22], methanol [23] and flourinated hydrocarbons [24] with the zirconia surface. Analysis of the chemical composition and electronic structure changes induced by 3-keV Ar^+ bombardment of thermally grown zirconia films has been reported [25–27]. These

* Corresponding author. Fax: +1-509-376-6066; e-mail: tm_orlando@pnl.gov or thomas.orlando@pnl.gov.

0039-6028/99/$ – see front matter
PII: S0039-6028(98)00908-X

studies concluded that Ar^+ bombardment induces the formation of oxygen vacancies and mixed metal oxidation states due to preferential sputtering of oxygen atoms. Similar studies using 1.0-keV He^+ and 2-keV electron-beam bombardment of yttria-stabilized ZrO_2 single crystals [28,29] report oxygen redistribution and loss.

It is well known that ion-, electron- and photon-bombardment leads to the desorption of surface bound species and material damage via electronic excitation processes [30]. Electron- and photon-stimulated desorption (ESD and PSD, respectively) are techniques that have been developed as excellent tools for identifying the dissociative electronic excitations that result in radiation damage in the near surface region. The stimulated desorption of O^+ from several full valency oxides can be described in terms of a multi-electron Auger-induced desorption mechanism. This was first proposed by Knotek and Feibelman (KF) to describe the ESD of O^+ from TiO_2 surfaces [31]. The ESD of cations from oxygen and hydrogen dosed Zr metal [32] and oxidized Zr/Ag [33] has been studied. In the latter case, the ratio of desorbing O atoms to O^+ was found to be higher than one would expect from the KF mechanism. Thus, Davidson et al. suggested that another model, involving a simpler single-electron desorption mechanism may be more appropriate to describe ESD from oxidized Zr/Ag [33].

None of the above mentioned radiation bombardment or ESD studies of zirconia specifically investigated the nature of the long-lived dissociative excitations which cause damage. Information on the dominant damage mechanisms can be obtained by measuring ESD and PSD threshold energies and ion kinetic energy distributions from undoped amorphous films and single crystal substrates. A direct comparison of the ESD and PSD from both surfaces also probes the role defects and the yttria dopant may have, if any, on the electronic desorption process. In this paper, we report a study of the ESD and PSD of cations from a thin film of amorphous ZrO_2 and a 9.5% yttria-stabilized $ZrO_2(100)$ single crystal. We also determine the electronic structures of these two samples using synchrotron-based soft X-ray photoelectron spectroscopy (SXPS). We find that O^+ is the primary ionic product from both samples and the onset for O^+ desorption corresponds primarily to excitation of the Zr(4p) core level, in accord with Auger-stimulated desorption of cations from metal oxide surfaces.

2. Experimental procedure

At room temperature, ZrO_2 is stable in the monoclinic phase and does not readily form large single crystals [34]. In order to have sufficiently large single crystals of zirconia, a dopant must be added, such as Y_2O_3, MgO or CaO, which stabilizes the cubic phase [34]. In the present experiments, we used single-crystal cubic zirconia samples ($10\,mm \times 10\,mm \times 0.5\,mm$) that were doped with 9.5 mol% Y_2O_3 and oriented along the (100) facet. The surfaces of the crystals were sputtered clean with an Ar^+ ion beam (0.5–3 keV), while being heated to ~ 500 K to prevent charging. The crystals were then annealed to ~ 900 K in vacuum or in a background pressure of O_2 ($\sim 10^{-5}$ Torr) to remove any Ar imbedded in the surface and to return the surface to a fully oxidized state. The ESD, PSD and SXPS measurements were carried out with the single crystal sample heated to 400–500 K, in order to prevent charging. Thermally induced phase segregation and extrinsic defect formation have not been observed in yttria-stabilized zirconia until temperatures which exceed 1000 K [35]. Oxygen vacancies are expected to hop at high temperatures (>1000 K) giving rise to high conductivity [36]. However, at temperatures below ~ 675 K, localization or association of vacancies begins to occur [36] and thus the use of substrate temperatures between 400 and 500 K is not expected to have significant effects on the ESD and PSD results.

For comparison with the doped crystals, undoped ZrO_2 films were grown on Zr foils (99.94% pure) that were sputtered clean then oxidized in situ via room-temperature exposure to O_2 (99.999% pure). Previous studies have shown that the oxidation of Zr rapidly saturates, forming 15–30 Å of oxide [6,7], after which oxidation slows considerably [7–10]. The amorphous films used in this study were grown with sufficient O_2 exposures

to attain this limiting thickness. The ESD, PSD and SXPS measurements on the oxidized foils were made at room temperature.

The ESD measurements were carried out at Pacific Northwest National Laboratory in an ultra-high vacuum chamber (base pressure 2×10^{-10} Torr) equipped with a low-energy electron gun, a quadrupole mass spectrometer (QMS), an ion sputter gun, and an Auger electron spectroscopy (AES) system. Sample cleanliness was determined using AES (see Ref. [3] for more details on sample cleaning and characterization). The ESD ions, generated by bombarding the zirconia surface with a mono-energetic beam of low-energy electrons (~3 nA/mm^2), were detected using the QMS, which had its ionizer turned off and its outermost element biased relative to the zirconia sample to enhance ion collection efficiency. Note that this configuration destroys any information regarding angular distributions of the desorbing ions. ESD excitation spectra were collected by monitoring the total ion yield in the QMS while varying the energy of the incident electron beam, and have been corrected to compensate for small variations in the electron beam current with energy. Under our low-current conditions the ESD ion yield is proportional to the incident electron current, indicating that the ions are produced directly with no contributions from gas-phase processes.

The SXPS measurements were carried out at beamline U8-a at the National Synchrotron Light Source at Brookhaven National Laboratory. The analysis chamber (base pressure 2×10^{-10} Torr) contains an angle-integrating ellipsoidal mirror analyzer [37] which was used to collect high-resolution photoelectron spectra, PSD excitation spectra, and PSD ion kinetic energy distributions. The photon energy was selected using a 3-m focal length grazing incidence toroidal grating monochromator. Sample cleanliness was determined from SXPS spectra, which compare well to clean-surface spectra reported by other groups [7,25,38,39]. The PSD excitation spectra were collected by ramping the photon energy while monitoring the total yield of cations using a pass energy which was several volts wide. The incident photon flux was also monitored during each measurement by collecting the photocurrent on the final focusing mirror. The SXPS and PSD data reported here are divided by the photocurrent intensity to scale out any variations in the measured signal arising from changes in the photon flux that occurred during the measurements. Note that the PSD measurements collect the total positive ion yield, and therefore are not mass-resolved. Care was taken to prepare the samples in the same manner as in the ESD measurements, which are mass-resolved and which identified the primary cation as O^+. Hence, we can say with some certainty that the predominant PSD cation is also O^+.

3. Results and discussion

Fig. 1 shows the thresholds for O^+ ESD from crystalline and amorphous zirconia. At the lowest electron energies, there is no detectable O^+ signal from the samples, which places an upper limit of $\sim10^{-23}$ cm^2 on the O^+ desorption cross section in this energy range [40]. For the cubic $ZrO_2(100)$ surface, the O^+ ESD begins to increase near 26–27 eV, with a very rapid increase above ~30 eV. For the amorphous zirconia surface, the O^+ ESD onset is somewhat more abrupt, with the ion yield increasing measurably at ~29–30 eV.

For the clean surfaces, O^+ is the predominant cation detected, although H^+, OH^+ and F^+ are

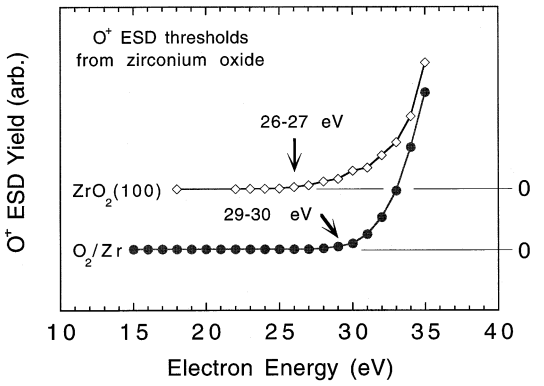

Fig. 1. Thresholds for the electron stimulated desorption (ESD) of O^+ ions from the surface of amorphous and cubic ZrO_2. The data, representing the O^+ yield as a function of incident electron energy, are offset vertically for display. The size of the symbols represents the estimated uncertainty in the measurements.

observed at considerably lower levels. If the surface is exposed to water vapor, however, then the H^+ and OH^+ ESD yields increase to levels comparable to that of O^+. Interestingly, the H^+ and OH^+ thresholds occur at around ~22–25 eV, several volts lower than for O^+ from the same surface (see Fig. 2). Knotek observed similar behavior in the ESD of cations from $TiO_2(100)$, from which he concluded that the O^+ threshold (31–32 eV) corresponds to the ionization of the Ti(3p) level while the onset for H^+ and OH^+ desorption (~21 eV) corresponds to the ionization of the O(2s) level, in each case through a multi-electron Auger decay process [41,42]. Considering the similarity in the results, it is reasonable to suggest that an Auger-stimulated desorption mechanism is involved in cation ESD from ZrO_2 as well.

To support this contention, we carried out a set of PSD experiments, measuring both thresholds and kinetic energy (KE) distributions of the desorbing ions. Fig. 3 shows the cation PSD excitation spectra for both cubic and amorphous zirconia. The threshold for the single crystal is ~31–32 eV and the threshold for the amorphous film is ~29–30 eV. This is the same (within our experimental error of ±1 eV) as the ESD threshold from the amorphous film. The PSD threshold for the cubic $ZrO_2(100)$ surface is, however, ~5 eV higher (~31–32 eV) than the ESD threshold (~26–27 eV).

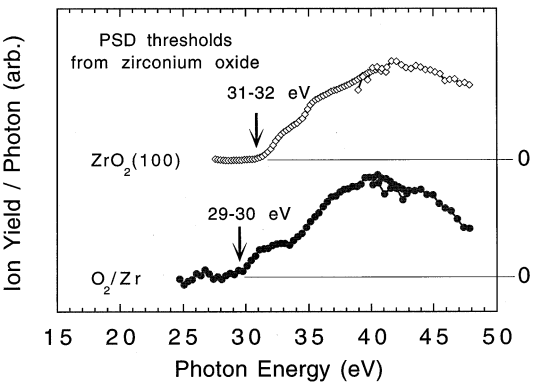

Fig. 3. Thresholds for the photon stimulated desorption (PSD) of positive ions from the surface of amorphous and cubic ZrO_2. The data, representing the ion yield as a function of incident photon energy, are offset vertically for display. The size of the symbols represents the estimated uncertainty in the measurements.

Fig. 4 shows the ion KE distributions collected from the same surfaces, using an incident photon energy of 70 eV, which is well above the desorption threshold. The KE distributions range from zero to ~7 eV, peaking at roughly 2 eV, indicating that the ions desorb with significant kinetic energy. There is a very small shoulder near 0.3 eV and some asymmetry at higher kinetic energies. The general KE distribution compares favorably with the distribution previously observed by Ashbury et al. when studying energy resolved ESD of

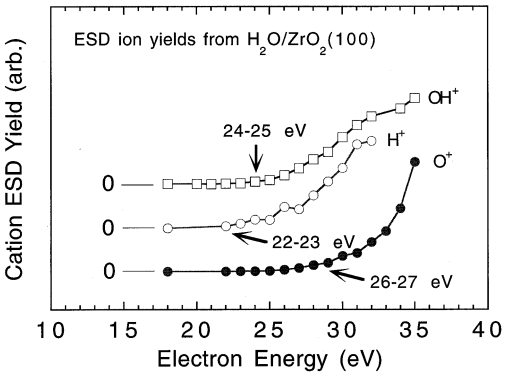

Fig. 2. Thresholds for the electron stimulated desorption (ESD) of O^+, H^+, and OH^+ ions from the surface of cubic ZrO_2 following exposure to water vapor. The data are offset vertically for display, and the size of the symbols represents the estimated uncertainty in the measurements.

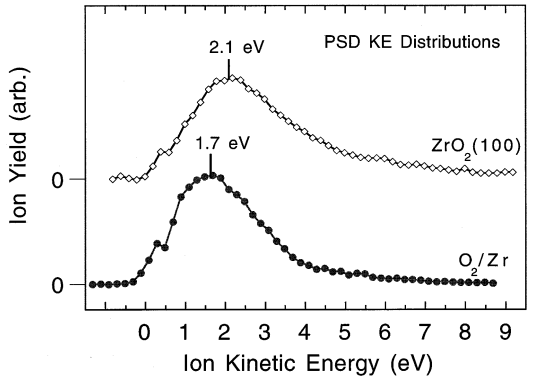

Fig. 4. The photon stimulated desorption (PSD) kinetic energy distributions of positive ions from the surface of amorphous and cubic ZrO_2. The data, representing the ion yield as a function of ion kinetic energy for a photon energy of 70 eV, are offset vertically for display.

hydrogen and oxygen dosed Zr metal [32]. Since the cation spectra are not mass resolved and it is rather difficult to prepare a completely hydrogen-free sample, it is reasonable to associate the small shoulder in Fig. 4 with the PSD of hydrogen ions. The H^+ has been shown by Ashbury et al [32] to desorb from hydrogen and oxygen dosed Zr metal with a lower kinetic energy distribution. The asymmetry and high energy tail is usually indicative of different O^+ ESD active binding sites [30].

In order to assign the primary excitation leading to O^+ desorption, we collected photoelectron spectra from the same surfaces. SXPS spectra of the amorphous and crystalline zirconia surfaces are shown in Fig. 5. The Zr(4s), Zr(4p) and O(2s) core levels are readily identified in both spectra. In addition, features assigned to the Y(4s) and Y(4p) core levels can be seen in the spectrum from the yttria-stabilized $ZrO_2(100)$ surface. Note that the amorphous oxide film is sufficiently thin (15–30 Å) that its spectrum has a measurable contribution from the unoxidized Zr metal substrate. This is most apparent in the valence region, which contains a significant contribution from the Zr(4d)-like conduction band of the underlying metal. The broadening of the Zr(4p) level in the spectrum of the oxidized foil, relative to that of the cubic crystal, also indicates that Zr atoms in the near-surface region are not all in the same oxidation state [25]. The high binding energy part

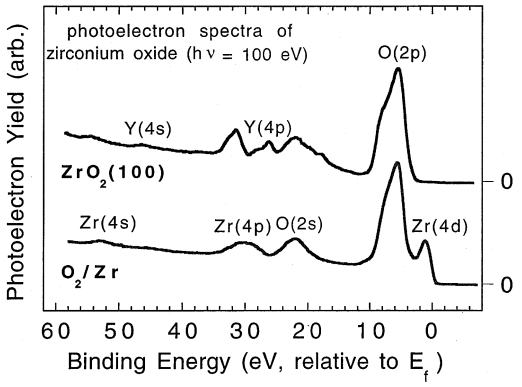

Fig. 5. Soft X-ray photoelectron spectra of the surface of amorphous and cubic ZrO_2 for a photon energy of 100 eV. The data, representing the photoelectron yield per incident photon, are offset vertically for display.

of the core level arises from fully oxidized Zr atoms in the film, while the low binding energy part arises from atoms in the metal substrate. It is also likely that some of the Zr atoms in the film, particularly those at the oxide/metal interface, are only partially oxidized [10,12–17]. The SXPS thin-film results (Fig. 5) are very consistent with previous electron-energy-loss measurements [15,43] and resonant photoemission studies [26] that report dominant features near 30 eV which are associated with transitions from the Zr(4p) band.

In assigning electronic transitions to the observed stimulated desorption thresholds, the simplest approach is to assume that the final state for a transition is the first significant density of unoccupied states. Note that since the valence band maximum is $\sim$4 eV below the Fermi level then the conduction band minimum should be about 1–1.5 eV above the Fermi level. There is also a reasonably high density of defect states in the gap associated with oxygen vacancies. The O^+ ESD and PSD thresholds for the oxidized foil are $\sim$29–30 eV, which we attribute to a transition from the Zr(4p) level of the (partially or fully) oxidized Zr atoms to the Fermi level. For the cubic crystal, the observed PSD) threshold of $\sim$31–32 eV is also consistent with ionization of the Zr(4p) level, with the conduction band as the final state.

Unfortunately, the nature of the lower 26–27 eV ESD threshold in cubic zirconia is less clear. A previous study with YSZ showed that, while zirconium atoms in the crystal are readily reduced from Zr^{4+} to Zr^0 by electron beam exposure, the dopant yttrium atoms are not reduced [29]. To explain this, Cotter and Egdell argued that, through an interatomic Auger decay mechanism, the difference in the covalency of the Zr–O and Y–O bonds leads to selective desorption of oxygen that is bonded to Zr [29]. Based on this, we expect no significant oxygen desorption to occur as a result of yttrium core level ionization. If, like all of the other thresholds, the initial state of the transition is the Zr(4p), then the final state must lie between the Fermi level and the conduction band minimum. Photoabsorption [44] and luminescence [45–47] studies have shown that a considerable density of states does exist in the band gap of this material

due to oxygen vacancies associated with the yttrium dopant. Therefore, the weak ESD onset below ~30 eV could be due to spin-forbidden transitions from the Zr(4p) core level to defect states in the gap, just below the conduction band minimum.

Finally, the difference between the ESD and PSD thresholds for YSZ may be due, at least in part, to contact potential differences between the electron gun and the samples, which can shift the ESD excitation spectra by ~1 eV or more. Assuming ESD and PSD have similar final states, a lower ESD threshold is expected due to the excess interaction energy which is available to the incoming electron but not the photon. The rapid rise in signal above ~31 eV would then correspond to a transition from the Zr(4p) to the conduction band. Hence, in all cases, the stimulated desorption of O^+ from zirconium oxide appears to be initiated by excitation of the Zr(4p) core level. For ZrO_2, oxygen is bound to the surface in the form of $O^{\delta-}$, where $\delta-$ is probably between 1 and 2, so the formation and ejection of an O^+ cation requires the removal of two or possibly three electrons from the same oxygen atom. A plausible explanation for how this occurs, through a multielectron Auger decay process, was first suggested by Knotek and Feibelman [31]. In their model a Zr(4p) core hole, formed by the impact of an incident electron or photon, is filled by a valence electron residing on a neighboring oxygen atom. To conserve energy, one or two additional Auger electrons are ejected from the same oxygen atom, leaving it in an O^0 or O^+ state, from which it desorbs. Once formed, O^+ ions have a strongly repulsive interaction with the surface, due to the reversal of the Madelung potential.

4. Conclusion

We investigated the photon- and electron-stimulated desorption of O^+ ions from amorphous ZrO_2 and cubic $ZrO_2(100)$ surfaces in order to understand the nature of the dominant dissociative excitations that occur in this material. For both types of zirconia, O^+ is the primary ionic desorption product. The threshold for ESD of O^+ from yttria-stabilized cubic zirconia (YSZ) is observed at ~26–27 eV with a rapid rise above ~30 eV. The PSD threshold from YSZ is $\sim 31 \pm 1$ eV. This is essentially the same as the O^+ ESD and PSD thresholds ($\sim 30 \pm 1$ eV) from undoped amorphous ZrO_2 surfaces. The kinetic energy of the ejected ions is also relatively high, ranging from zero to 7 eV, peaking at around 2 eV. By comparing the ion desorption thresholds to photoelectron spectra collected from the same surfaces, we determined that excitation of the Zr(4p) core level initiates O^+ desorption. All of this evidence suggests that in ZrO_2, O^+ is produced via a multielectron Auger-stimulated desorption mechanism.

5. Note added in proof

The data in Fig. 3 suggests that stimulated desorption of O^+ from YSZ and thin amorphous ZrO_2 films may involve the Zr(4p→4d) and Zr(4p→5sp) core excitons as *initial* excitations. These core excitons, which are peaked at ~39 and between 40–50 eV, respectively, can relax via recombination processes involving valence bands with metal admixtures. The *final* hole states will be the same as those produced via direct photoemission and O^+ desorption should proceed via a multielectron Auger process as discussed in the text.

Acknowledgements

This work was supported by the US Department of Energy, Environmental Management Science Program, and by the US Department of Energy (DOE), Office of Basic Energy Sciences, Chemical Physics Program. The W.R. Wiley Environmental Molecular Sciences Laboratory, a national scientific user facility sponsored by the DOE Office of Biological and Environmental Research, is located at the Pacific Northwest National Laboratory (PNNL). PNNL is operated by Battelle Memorial Institute under contract no. DE-AC06-76RLO-1830. WCS is an Associated Western Universities Postdoctoral. Fellow, supported under Grant

DE-17G07-94ID-13228 with the US Department of Energy.

References

[1] S. Jiang, W.A. Schulze, G.C. Stange, J. Mater. Res. 12 (1997) 2374.
[2] G. Lu, N. Miura, N. Yamazoe, J. Mater. Chem. 7 (1997) 1445.
[3] D.P. Taylor, W.C. Simpson, K. Knutsen, M.A. Henderson, T.M. Orlando, Appl. Surf. Sci. 127–129 (1998) 101.
[4] N. Mansour, K. Mansour, E.W.V. Stryland, M.J. Soileau, J. Appl. Phys. 67 (1989) 1475.
[5] C. Lemaignan, J. Nucl. Mater. 187 (1992) 122.
[6] Y. Nishino, A.R. Krauss, Y. Lin, D.M. Gruen, J. Nucl. Mater. 228 (1996) 346.
[7] R.L. Tapping, J. Nucl. Mater. 107 (1982) 151.
[8] J.S. Foord, P.J. Goddard, R.M. Lambert, Surf. Sci. 94 (1980) 339.
[9] G.B. Hoflund, G.R. Corallo, D.A. Asbury, R.E. Gilbert, J. Vac. Sci. Technol. A 5 (1987) 1120.
[10] C.-S. Zhang, B.J. Flinn, P.R. Norton, Surf. Sci. 264 (1992) 1.
[11] G.R. CoralloY, D.A. Asbury, R.E. Gilbert, G.B. Hoflund, Phys. Rev. B 35 (1987) 9451.
[12] C.O. De González, E.A. Garcia, Surf. Sci. 193 (1988) 305.
[13] G. Hoflund, Y.D.A. Asbury, D.F. Cox, R.E. Gilbert, Appl. Surf. Sci. 22/23 (1985) 252.
[14] G.N. Krishnan, B.J. Wood, D. Cubicciotti, J. Electrochem. Soc. 128 (1981) 191.
[15] L. Kumar, D.D. Sarma, S. Krummacher, Appl. Surf. Sci. 32 (1988) 309.
[16] V. Maurice, M. Salmeron, G.A. Somorjai, Surf. Sci. 237 (1990) 116.
[17] C. Morant, J.M. Sanz, L. Galán, L. Soriano, F. Rueda, Surf. Sci. 218 (1989) 331.
[18] C. Palacio, J.M. Sanz, J.M. Martinez-Duart, Surf. Sci. 191 (1987) 385.
[19] T. Tanabe, M. Tomita, Surf. Sci. 222 (1989) 84.
[20] M. Tomita, T. Tanabe, S. Imoto, Surf. Sci. 209 (1989) 173.
[21] M. Yamamoto, S. Naito, M. Mabuchi, T. Hashino, J. Chem. Soc. Faraday Trans. 87 (1991) 1591.
[22] B. Li, K. Griffiths, C.A. Zhang, P.R. Norton, Surf. Sci. 370 (1997) 97.
[23] P.A. Dilara, J.M. Vohs, Surf. Sci. 321 (1994) 8.
[24] K. Takeuchi, S.S. Perry, M. Salmeron, G.A. Samorjai, Surf. Sci. 323 (1995) 30.
[25] C. Morant, J.M. Sanz, L. Galán, Phys. Rev. B 45 (1992) 1391.
[26] C. Morant, A. Fernández, A.R. González-Elipe, L. Soriano, A. Stampfl, A.M. Bradshaw, J.M. Sanz, Phys. Rev. B 52 (1995) 11711.
[27] J.M. Sanz, A.R. González-Elipe, A. Fernández, D. Leinen, L. Galán, A. Stampfl, A.M. Bradshaw, Surf. Sci. 307 (1994) 848.
[28] V.A. Miteva, A. Stanchev, Y. Marashev, R. Kelly, A. Licciardello, Vacuum 47 (1996) 1235.
[29] M. Cotter, R.G. Egdell, J. Solid State Chem. 66 (1987) 364.
[30] R.D. Ramsier, J.T. Yates, Surf. Sci. Rep. 12 (1991) 243.
[31] M.L. Knotek, P.J. Feibelman, Phys. Rev. Lett. 40 (1978) 964.
[32] D.A. Asbury, G.B. Hoflund, W.J. Peterson, R.E. Gilbert, R.A. Outlaw, Surf. Sci. 185 (1987) 213.
[33] M.R. Davidson, G.B. Hoflund, R.A. Outlaw, Surf. Sci. 281 (1993) 111.
[34] A.L. Shluger, A.H. Harker, R.W. Grimes, C.R.A. Catlow, Phil. Trans. R. Soc. Lond. A 341 (1992) 221.
[35] A.E. Hughes, J. Am. Ceram. Soc. 78 (1995) 369.
[36] C. Leon, M.L. Lucia, J. Santamaria, Phys. Rev. B 55 (1997) 882.
[37] D.E. Eastman, J.J. Donelon, N.C. Hien, F.J. Himpsel, Nucl. Instrum. Meth. 172 (1980) 327.
[38] P. Camagni, G. Samoggia, L. Sangaletti, F. Parmigiani, N. Zema, Phys. Rev. B 50 (1994) 4292.
[39] B.W. Veal, D.J. Lam, D.G. Westlake, Phys. Rev. B 19 (1979) 2856.
[40] K. Knutsen, T.M. Orlando, Surf. Sci. 348 (1996) 143.
[41] M.L. Knotek, Surf. Sci. 91 (1980) L17.
[42] M.L. Knotek, Surf. Sci. 101 (1980) 334.
[43] M. Kurahashi, M. Yamamoto, M. Mabuchi, S. Naito, J. Phys.: Condens. Matter 7 (1995) 4763.
[44] V.R. PaiVemeker, A.N. Petelin, F.J. Crowne, D.C. Nagle, Phys. Rev. B 40 (1989) 8555.
[45] S.E. Paje, J. Llopis, Appl. Phys. A 57 (1993) 225.
[46] S.E. Paje, J. Llopis, J. Phys. Chem. Solids 55 (1994) 671.
[47] N.G. Petrik, D.P. Taylor, T.M. Orlando, J. Appl. Phys., in press.